Journal of Zhejiang University-SCIENCE A (Applied Physics & Engineering)
ISSN 1673-565X (Print); ISSN 1862-1775 (Online)
www.zju.edu.cn/jzus; www.springerlink.com
E-mail: jzus@zju.edu.cn

# Experimental evaluation of the effect of an internal heat exchanger on a transcritical $CO_2$ ejector system*

Xiao-xiao XU†, Guang-ming CHEN†‡, Li-ming TANG, Zhi-jiang ZHU, Shuang LIU

(*Institute of Refrigeration and Cryogenics, State Key Laboratory of Clean Energy Utilization, Zhejiang University, Hangzhou 310027, China*)

†E-mail: xuxiaoxiao19@126.com; gmchen@zju.edu.cn

Received May 5, 2010; Revision accepted July 22, 2010; Crosschecked Jan. 6, 2011

**Abstract:** This study presents experimental results focused on a performance comparison of a transcritical $CO_2$ ejector system without an internal heat exchanger (IHX) (EJE-S) to a transcritical $CO_2$ ejector system with an IHX (EJE-IHX-S). The comparison includes the effects of changes in operating conditions such as cooling water flow rate and inlet temperature. Experiments are conducted to assess the influence of the IHX on the heating coefficient of performance ($COP_r$), heating capacity, entrainment ratio, pressure lift, and other parameters. The primary flow rate of the EJE-IHX-S is higher than that of the EJE-S. The pressure lift and actual ejector work recovery are reduced when the IHX is added to the transcritical $CO_2$ ejector system. Using a more practical performance calculation, the compression ratio in the EJE-S is reduced by 10.0%–12.1%, while that of EJE-IHX-S is reduced only by 5.6%–6.7% compared to that of a conventional transcritical $CO_2$ system. Experimental results are used to validate the findings that the IHX weakens the contribution of the ejector to the system performance.

**Key words:** $CO_2$ ejector system, Transcritical cycle, Heating coefficient of performance ($COP_r$)
**doi:**10.1631/jzus.A1000212 **Document code:** A **CLC number:** TB61

## 1 Introduction

Since Lorentzen and Pettersen (1993) proposed the transcritical $CO_2$ cycle for mobile air-conditioning applications, a number of cycle improvements such as multistage compression with intercooling, throttling loss reduction through internal heat exchange, and expansion work recovery have been performed. Among these cycle improvements, the effects of an internal heat exchanger (IHX) for transcritical automotive air-conditioning systems with $CO_2$ as a working fluid have been studied by many researchers. The IHX lowers the optimum high-side pressure for maximizing system performance as discussed by Kim *et al.* (2004), and the cycle coefficient of performance (COP) was further increased by higher compressor efficiencies as a result of reduced compression ratios in a conventional system. Mu *et al.* (2003) also showed that larger IHX capacity can lower the optimum high-side pressure. Aprea and Maiorino (2008) performed an experimental comparison of a transcritical $CO_2$ system working with and without an IHX. They showed the cycle with an IHX had a COP improvement of up to 10 % over the cycle without an IHX. Results presented by Boewe *et al.* (2001) also indicated COP improvements up to 25% over the cycle without an IHX. Tao *et al.* (2010) proposed that the IHX can reduce the throttling loss of the transcritical $CO_2$ cycle. Chen and Gu (2005) derived a practical effectiveness expression for the IHX based on enthalpy difference, and reported theoretically that an IHX with high effectiveness was an important factor in achieving a high system performance in the transcritical $CO_2$ cycle.

All the above studies focused on the transcritical $CO_2$ system. For the transcritical $CO_2$ ejector system (EJE-S), Elbel and Hrnjak (2004) performed a

‡ Corresponding author

* Project supported by the National Basic Research Program (973) of China (No. 2010CB227304), and the National Key Technologies R & D Program in China (No. 2006BAJ01A10)

detailed theoretical investigation, and showed that the IHX can improve the COP of an EJE-S in comparison to its counterpart without an IHX. In addition, a thermodynamic property chart to illustrate the interference between expansion work recovery and IHX was provided by Elbel and Hrnjak (2006). Later experimental results confirmed that the highest COP was achieved with an ejector and a high IHX effectiveness (Elbel and Hrnjak, 2008). The theoretical work of Robinson and Groll (1998) showed that use of an IHX in conjunction with a work recovery device degraded the performance of the work recovery turbine cycle, while the use of an IHX in conjunction with an expansion valve increased the COP. It seems interesting to undertake some work to investigate the existing trade-off between an IHX and an ejector in an EJE-S, but the available literature contains far more numerical studies than experimental investigations. In order to investigate the effects of the IHX on the EJE-S, this paper presents experimental research focused on a comparison of the EJE-S and the EJE-S with an IHX (EJE-IHX-S) under identical working conditions. The influence of the IHX on the heating coefficient of performance ($COP_r$), heating capacity, entrainment ratio, pressure lift, and other parameters are analyzed. In addition, a more practical performance metric, the compression ratio, is introduced to assess the effects of an IHX on ejector system performance.

## 2 Experiments

The schematic of a prototype transcritical $CO_2$ system (Fig. 1) shows the main components of the system: a reciprocating compressor, a gas-cooler, an evaporator, an IHX, an ejector, and a liquid-vapor separator. The prototype system is designed and built based on a residential $CO_2$ heat pump water heater with a 12 kW heating capacity.

A Dorin $CO_2$ reciprocating compressor (TCS 340/4-D) was used in the system, with a theoretical swept volume of 3.5 $m^3$/h. A two-phase fixed ejector was designed and built for the transcritical $CO_2$ heat pump system. The details of the design processes followed Liu (2008). The dimensions of the helical-coil-in-fluted-tube gas cooler are given in Table 1. The gas cooler consisted of helically coiled tubes and fluted tubes. It was fabricated by twisting a straight copper tube into a helically coiled tube, and then embedded in the groove of the fluted tube. Refrigerant $CO_2$ and water were used as working fluids in the helical-coil tube and the fluted tube, respectively. The evaporator and the IHX adopted a tube-in-tube heat exchanger construction. The $CO_2$ refrigerant flowed in the inner tube, and cold water flowed in the annulus in a counter flow configuration. The evaporator and the IHX specifications are summarized in Table 2. The cooling water and the chilled water in the tank were heated with an electric heater and supplied

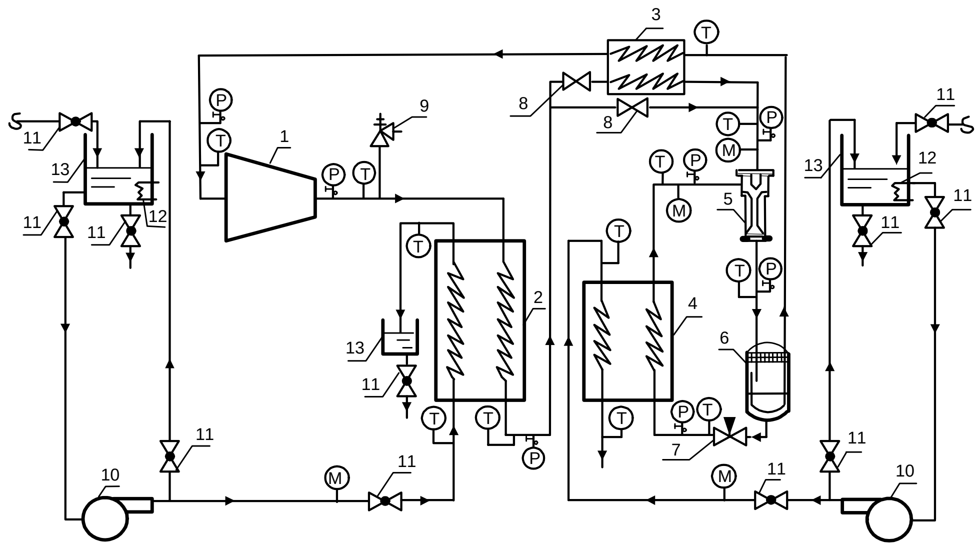

**Fig. 1 Schematic diagram of experimental apparatus**

1: compressor; 2: gas cooler; 3: internal heat exchanger (IHX); 4: evaporator; 5: ejector; 6: liquid-vapor separator; 7: metering valve; 8: cut-off valve; 9: relief valve; 10: pump; 11: ball valve; 12: electrical heater; 13: water tank. T: temperature; P: pressure; M: mass flow rate

**Table 1 Characteristics of the helical-coil-in-fluted- tube gas cooler**

| Type | Number | OD (mm) | ID (mm) | Wall thickness (mm) | $L$ (mm) | $L_{total}$ (mm) | Fluted depth (mm) | Number of fluted starts | Fluted pitch (mm) | Helix angle (°) |
|---|---|---|---|---|---|---|---|---|---|---|
| Fluted tube | 2 | 17 | 15.0 | 1.00 | 6750 | 13500 | 4 | 4 | 6 | 65.8 |
| Helical-coil tube | 8 | 4 | 2.5 | 0.75 | 16200 | 129600 | | | | |

OD and ID are the volumes based outer diameter and inner diameter, respectively; $L$ is the length of a single tube, and $L_{total}$ is the total length of all tubes

**Table 2 Heat exchanger specifications**

| Heat exchanger | Material of tube | Inner tube (mm) | Outer tube (mm) | Length of tube (m) | Number of tube |
|---|---|---|---|---|---|
| Evaporator | Copper | Φ8×1 | Φ14×1 | 4 | 4 |
| IHX | Copper | Φ8×1 | Φ14×1 | 5 | 4 |

IHX: internal heat exchanger

through the gas cooler and evaporator, respectively. Comparing the measured valve and the setting value of the two tank temperatures, the heating power of the electrical heater was controlled by the temperature control unit. The control accuracy of the cooling water temperature and the chilled water temperature was within ±0.3 °C.

The system was capable of operating in two cycles: the EJE-IHX-S and the EJE-S. The mode of operation was selected by switching cut-off valve. There were two approaches to compare the system performance for the two modes of operation. One was based on internal parameters, i.e., evaporating and condensing temperatures. The two modes of operation were compared under the same evaporating and condensing temperatures. The other one shown in Hoegberg *et al.* (1993) was based on external parameters such as the inlet temperature and the flow rate of the heat transfer fluid. This method allowed each mode of operation to operate under the same external conditions. Giuliani *et al.* (1999) proposed that the latter method was more likely in real life. In this study, changes in the operating conditions of cooling water flow rate and inlet temperature were selected to evaluate the effects of IHX on the EJE-S. The operating conditions were as follows:

1. The effects of the cooling water flow rates on the performance of the EJE-IHX-S and the EJE-S were explored by setting the volumetric flow rates of the cooling water at 4.2, 3.7, 3.4, 3.1, and 2.7 L/min, while the cooling water temperature and chilled water temperature were kept constant at 17 °C, and the volumetric flow rate of the chilled water was fixed at 22 L/min.

2. The effects of the cooling water inlet temperature on the performance of the EJE-IHX-S and the EJE-S were explored by setting the cooling water inlet temperatures to 18, 20, 22, 24, and 26 °C, while the volumetric flow rate was kept constant at 4 L/min, and the volumetric flow rate and inlet temperature of the chilled water were fixed at 22 L/min and 17 °C, respectively.

The $CO_2$ and water temperatures were measured using type-T thermocouples with an accuracy of ±0.5 °C and ±0.3 °C, respectively. GE Druck PTX7517 absolute pressure transducers with a range of 0–16 MPa were used, with an uncertainty of ±0.2% full scale (FS). The $CO_2$ mass flow rate was measured with an Emerson Micro Motion mass flow meter located at the motive nozzle inlet and suction nozzle inlet of the ejector, with a reading uncertainty of ±0.1%. The water flow rates in the gas cooler and evaporator were measured using a rotometer with an accuracy of ±0.2% FS. The compressor electrical power consumption was measured using a digital wattmeter, with an uncertainty of ±0.5% FS. All the data acquisition systems were computer controlled and recorded, and a sampling rate of 0.5 Hz was used for each channel; steady state conditions were assumed to prevail whenever all measurements varied by less than the experimental uncertainty for 90 consecutive readings, and averages of 30 readings were used in the data reduction.

The heating capacity was determined from the Coriolis-type mass flow meter measurement, and the specific enthalpies across the gas cooler were all recorded for the refrigerant flow. The heating capacity $Q_r$ was calculated by

$$Q_r = m_P(h_{gc,in} - h_{gc,out}), \quad (1)$$

where $m_P$ is the primary mass flow rate of the refrigerant $CO_2$ of the gas cooler, and $h_{gc,in}$ and $h_{gc,out}$ are the inlet and outlet enthalpies of the gas cooler, respectively.

The $COP_r$ is defined as

$$COP_r = Q_r/W, \tag{2}$$

where $W$ is the electrical power supplied to the compressor.

To explore changes in the ejector performance when an IHX was added to the EJE-S, the ejector parameters were introduced. The entrainment ratio $u$ and pressure lift $p_{lift}$ of the ejector are defined as

$$u = m_H/m_P, \tag{3}$$

$$p_{lift} = p_C/p_H, \tag{4}$$

and the actual ejector work recovery $W_{actual}$ is defined according to Elbel and Hrnjak (2008):

$$W_{actual} = m_H \Delta h_{actual}, \tag{5}$$

where $m_H$ is the entrained mass flow rate of the refrigerant $CO_2$ of the evaporator; $p_C$ is the back pressure (the ejector outlet pressure); $p_H$ is the entrained flow pressure (the evaporator pressure); and $\Delta h_{actual}$ is the actual enthalpy change required to reach the condition of the ejector outlet from the evaporation pressure assuming isentropic compression.

For the water-side and refrigerant-side balances, the measured heating capacity and the $COP_r$ typically had range uncertainties of ±4.2%–±5.9% and ±3.3%–±4.0%, respectively. Table 3 provides the uncertainties in the experimental results.

**Table 3 Range of uncertainties of calculated parameters**

| Parameter | Range of uncertainties (%) |
|---|---|
| Entrainment ratio | ±1.5–±1.8 |
| Pressure lift | ±0.9–±1.4 |
| Ejector actual work recovery | ±1.2–±1.8 |
| Compression ratio, $p_{PC}$ | ±1.3–±2.3 |
| Compression ratio, $p_{PH}$ | ±1.5–±2.8 |
| Heating capacity | ±4.2–±5.9 |
| Heating coefficient of performance | ±3.3–±4.0 |

$p_{PH}$ and $p_{PC}$ are the ratios between the compressor discharge pressure and the entrained flow pressure or back pressure, respectively

## 3 Results and discussion

As shown in Table 4, the gas cooler outlet pressure $p_{gc,out}$, the gas cooler outlet temperature $T_{gc,out}$, the compressor suction temperature $T_{suc}$, the outlet temperature of the IHX $T_{IHX,out}$ (high pressure side), and the evaporating temperature $T_e$ increased as the cooling water flow rate $m_w$ decreased or the inlet temperature $T_{w\_in}$ increased in the EJE-S and the EJE-IHX-S. It can also be observed that the gas cooler outlet temperature $T_{gc,out}$ for the EJE-IHX-S was lower than that for the EJE-S. Furthermore, the evaporating temperature $T_e$ in the EJE-IHX-S was at least 10 °C higher than that in the EJE-S.

The effects of the cooling water flow rate and the inlet temperature on the ejector performance parameters for the EJE-S with and without an IHX are shown in Table 5. The EJE-IHX-S has a higher primary flow rate than the EJE-S, which acted counter to the influence of the IHX on the conventional refrigeration system. The reason was that the compressor suction temperature increases through the IHX, while the compressor suction pressure rose at the same time. Therefore, the effect of the IHX on the specific volumes at the compressor suction was small. However, the specific volumes at the compressor discharge increased through the IHX, resulting in an increase of the compressor volumetric efficiency according to the equation, which was presented in Klein *et al.* (2000):

$$\eta_v = 1 - R\left(\frac{v_{suc}}{v_{dis}} - 1\right), \tag{6}$$

where $\eta_v$ is the compressor volumetric efficiency, $R$ is the ratio of the clearance volume to the displacement volume, and $v_{suc}$ and $v_{dis}$ are the refrigerant specific volumes at the compressor suction and discharge, respectively. Thus, in comparison to the EJE-S, the primary flow rate in the EJE-IHX-S increased.

As shown in Table 5, the entrainment ratio and the pressure lift also increase for the EJE-S and the EJE-IHX-S as the cooling water flow rate decreases or the inlet temperature increases. Note that the entrainment ratio increases in the EJE-IHX-S, while the pressure lift was reduced, compared to that of the EJE-S. This effect was mainly caused by the increase

**Table 4 Trends of main temperature parameters and gas cooler outlet pressure for different cooling water flow rates and inlet temperatures with and without the IHX**

| $m_w$ (L/min) ($T_{w\_in}$=17 °C) | $p_{gc,out}$ (MPa) | | $T_{gc,out}$ (°C) | | $T_{IHX,out}$ (°C) | $T_{suc}$ (°C) | | $T_e$ (°C) | |
|---|---|---|---|---|---|---|---|---|---|
| | With the IHX | Without the IHX | With the IHX | Without the IHX | With the IHX | With the IHX | Without the IHX | With the IHX | Without the IHX |
| 4.2 | 7.205 | 8.148 | 26.8 | 29.0 | 21.8 | 21.5 | −0.6 | 5.8 | −4.4 |
| 3.7 | 7.540 | 8.444 | 28.8 | 30.6 | 23.0 | 23.0 | 0.1 | 7.2 | −3.9 |
| 3.4 | 7.857 | 8.709 | 30.7 | 31.9 | 24.1 | 24.5 | 0.8 | 8.4 | −3.0 |
| 3.1 | 8.338 | 9.078 | 33.8 | 34.0 | 26.1 | 26.9 | 1.5 | 9.7 | −2.3 |
| 2.7 | 8.703 | 10.02 | 36.4 | 39.1 | 27.8 | 27.8 | 3.5 | 10.7 | 0.2 |
| $T_{w\_in}$ (°C) ($m_w$=4 L/min) | $p_{gc,out}$ (MPa) | | $T_{gc,out}$ (°C) | | $T_{IHX,out}$ (°C) | $T_{suc}$ (°C) | | $T_e$ (°C) | |
| | With the IHX | Without the IHX | With the IHX | Without the IHX | With the IHX | With the IHX | Without the IHX | With the IHX | Without the IHX |
| 18 | 7.327 | 8.703 | 27.2 | 31.8 | 21.4 | 21.0 | 1.0 | 7.3 | −2.8 |
| 20 | 7.639 | 8.903 | 28.9 | 33.2 | 22.4 | 22.4 | 1.2 | 8.0 | −2.7 |
| 22 | 7.906 | 9.145 | 30.4 | 34.4 | 23.3 | 23.4 | 1.6 | 8.8 | −2.2 |
| 24 | 8.089 | 9.393 | 31.4 | 35.8 | 23.9 | 24.2 | 2.1 | 9.2 | −1.3 |
| 26 | 8.533 | 9.707 | 34.3 | 37.5 | 25.7 | 26.3 | 2.5 | 10.2 | −0.9 |

$m_w$: cooling water flow rate; $T_{w\_in}$: cooling water inlet temperature; $p_{gc,out}$: gas cooler outlet pressure; $T_{gc,out}$: gas cooler outlet temperature; $T_{IHX,out}$: IHX outlet temperature; $T_{suc}$: compressor suction temperature; $T_e$: evaporating temperature

**Table 5 Trends of ejector parameters for different cooling water flow rates and inlet temperatures with and without the IHX**

| $m_w$ (L/min) ($T_{w\_in}$=17 °C) | $m_P$ (kg/s) | | $u$ | | $p_{lift}$ | | $W_{actual}$ (kW) | |
|---|---|---|---|---|---|---|---|---|
| | With the IHX | Without the IHX | With the IHX | Without the IHX | With the IHX | Without the IHX | With the IHX | Without the IHX |
| 4.2 | 0.075 | 0.065 | 0.600 | 0.615 | 1.061 | 1.110 | 0.104 | 0.182 |
| 3.7 | 0.076 | 0.066 | 0.618 | 0.621 | 1.063 | 1.116 | 0.108 | 0.195 |
| 3.4 | 0.078 | 0.067 | 0.628 | 0.627 | 1.065 | 1.116 | 0.113 | 0.199 |
| 3.1 | 0.079 | 0.069 | 0.646 | 0.638 | 1.069 | 1.125 | 0.118 | 0.223 |
| 2.7 | 0.080 | 0.075 | 0.663 | 0.640 | 1.070 | 1.138 | 0.120 | 0.261 |
| $T_{w\_in}$ (°C) ($m_w$ =4 L/min) | $m_P$ (kg/s) | | $u$ | | $p_{lift}$ | | $W_{actual}$ (kW) | |
| | With the IHX | Without the IHX | With the IHX | Without the IHX | With the IHX | Without the IHX | With the IHX | Without the IHX |
| 18 | 0.076 | 0.068 | 0.605 | 0.603 | 1.060 | 1.119 | 0.100 | 0.200 |
| 20 | 0.077 | 0.069 | 0.623 | 0.609 | 1.063 | 1.124 | 0.107 | 0.213 |
| 22 | 0.078 | 0.070 | 0.628 | 0.614 | 1.064 | 1.127 | 0.109 | 0.221 |
| 24 | 0.078 | 0.071 | 0.641 | 0.620 | 1.066 | 1.128 | 0.111 | 0.227 |
| 26 | 0.079 | 0.072 | 0.658 | 0.625 | 1.069 | 1.137 | 0.117 | 0.246 |

$m_w$: cooling water flow rate; $T_{w\_in}$: cooling water inlet temperature; $m_P$: primary flow rate; $u$: entrainment ratio; $p_{lift}$: pressure lift; $W_{actual}$: actual ejector work recovery

of the primary flow rate, which entrained more of the entrained flow when the IHX was added into the EJE-S. The lower primary flow pressure in the EJE-IHX-S resulted in the reduced pressure lift.

In addition, it can be observed that the actual ejector work recovery was reduced in the EJE-IHX-S as compared to the EJE-S, because the primary flow entering the IHX had a lower specific enthalpy. There existed an interference between the IHX and the ejector; that is, the IHX reduced the actual ejector work recovery.

The effects of the cooling water flow rate and the inlet temperature on compression ratio when the EJE-S runs with and without an IHX are shown in Fig. 2. In order to apply a more intuitive way to define the effect of IHX on the $CO_2$ ejector system performance, the compression ratios $p_{PH}$ and $p_{PC}$ were introduced. The ratio between the compressor discharge pressure and the entrained flow pressure was named $p_{PH}$, which was an equivalent form of the compression ratio of the conventional transcritical $CO_2$ cycle. The ratio between the compressor discharge pressure and back pressure was named $p_{PC}$, which was an equivalent form of the compression ratio of the transcritical $CO_2$ ejector cycle. The above two compression ratios were calculated by ignoring the pressure losses of $CO_2$ flowing from the ejector outlet to compressor suction, and ignoring the inconsistency of the primary flow rate and the entrained flow rate.

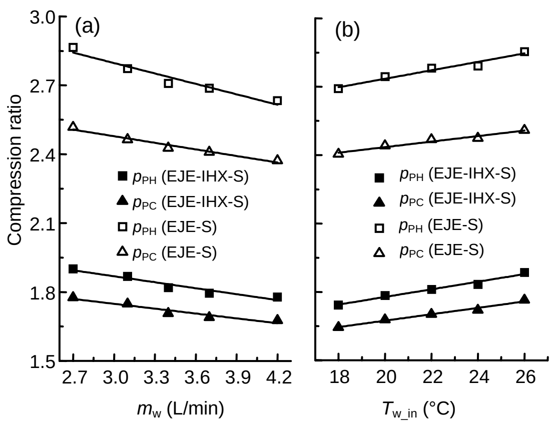


**Fig. 2 Trends of compression ratios for different cooling water flow rates $m_w$ (a) and inlet temperatures $T_{w\_in}$ (b) with and without the IHX**

As shown in Fig. 2, $p_{PC}$ and $p_{PH}$ increase when the cooling water flow rate decreases or the inlet temperature increases in the EJE-S and the EJE-IHX-S. The $p_{PC}$ and $p_{PH}$ of the EJE-IHX-S were all lower than those of the EJE-S, which demonstrated that the use of the IHX reduced the compression ratio. This finding agreed with the result that the IHX lowered the performance maximizing high-side pressure in transcritcal $CO_2$ cycle as discussed by Kim *et al.* (2004). The reduced compression ratio produced higher compressor efficiency, and thus, the $COP_r$ of the EJE-IHX-S can be further improved. Compared to that of a conventional transcritical $CO_2$ system, the compression ratio in the EJE-S was reduced 10.0%–12.1%, whereas $p_{PC}$ was only 5.6%–6.7% lower than $p_{PH}$ in the EJE-IHX-S. Experimental results validated that an interference existed between the IHX and the ejector. The IHX improved the EJE-S performance but weakened the contribution of the ejector to the system performances.

The effects of the cooling water flow rate and the inlet temperature on heating capacity when the EJE-S runs with and without IHX are shown in Fig. 3. As the cooling water flow rate decreased or the inlet temperature increased, the heating capacities in the EJE-S and the EJE-IHX-S were reduced due to the smaller enthalpy difference across the gas cooler resulting from a higher outlet temperature of the gas cooler (Table 4). Although an increase in the primary flow rate was associated with an increase in the heat transfer coefficient of the gas cooler, a decrease in the flow rate of the cooling water or an increase in the inlet temperature of the cooling water directly caused the heat transfer coefficient of gas cooler to decrease. Overall, the cooling water flow rate and the inlet temperature had a positive effect on heating capacity apparently outweighing the primary flow rate, and thus the heating capacity decreased.

As shown in Fig. 3, the heating capacity of the EJE-IHX-S was higher than that of the EJE-S. There are two main reasons. The first was that the use of the IHX led to an increase of the primary flow rate, and the second was that the gas cooler outlet temperature of the EJE-IHX-S was lower than that of the EJE-S (Table 4). Our conjecture was that this behavior was partly due to the increased primary flow rate in the EJE-IHX-S as a consequence of the higher heat transfer coefficient of the gas cooler and its related increase in heating capacity at given gas cooler dimensions.

The effects of cooling water flow rate and inlet temperature on $COP_r$ when the EJE-S runs with and without IHX are shown in Fig. 4. As the cooling water flow rate decreased or the inlet temperature increased, the $COP_r$ decreased in the EJE-S and the EJE-IHX-S.

The use of an IHX can not only further reduce the compression ratio (Fig. 2), but also increase the heating capacity (Fig. 3). The IHX had a positive effect on the system performance, and there was still the possibility to enhance the ejector efficiency. Furthermore, the low ejector efficiency was associated with the structure of helical-coil-in-fluted-tube gas cooler. The large pressure drop in the gas cooler lost a part of pressure energy to drive more entrained flow, even though the gas cooler had a high heat transfer efficiency. Therefore, the optimal matching of the ejector and system components was also a key factor for improving system performance.

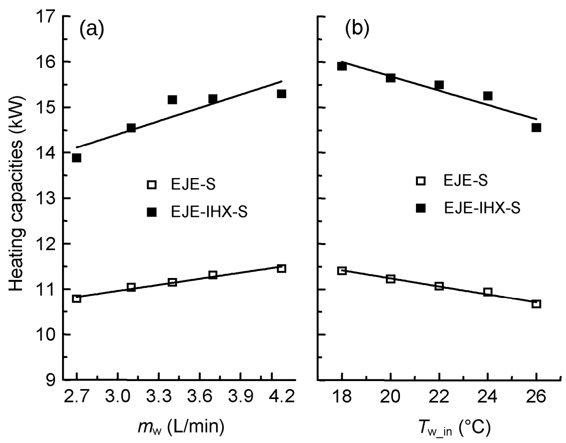


**Fig. 3 Trends of heating capacities for different cooling water flow rates $m_w$ (a) and inlet temperatures $T_{w\_in}$ (b) with and without the IHX**

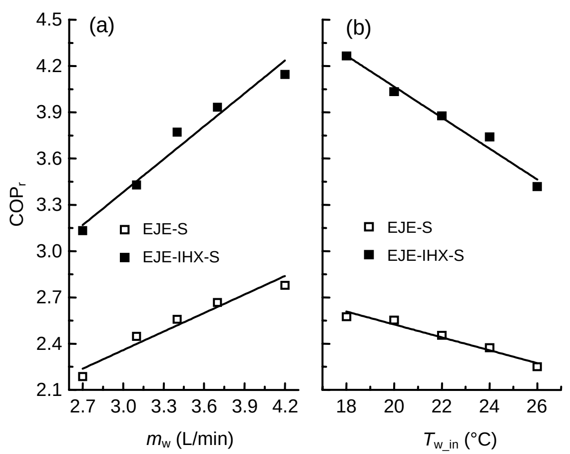


**Fig. 4 Trends of heating coefficients of performance $COP_r$ for different cooling water flow rates $m_w$ (a) and inlet temperatures $T_{w\_in}$ (b) with and without the IHX**

## 4 Conclusions

A performance comparison between the EJE-IHX-S and the EJE-S under identical conditions is investigated experimentally. Results reveal the influence of the IHX on the EJE-S. It is found that the IHX used in an ejector system differs greatly from that in a conventional system. Unlike in a conventional system with an expansion valve, the primary flow rate of the EJE-IHX-S is higher than that of the EJE-S. Experiments show that the entrainment ratio and the pressure lift increase for the EJE-S and the EJE-IHX-S, with a decrease in cooling water flow rate or an increase in the inlet temperature. It is also found that the pressure lift and the actual ejector work recovery are reduced when the IHX is added to the EJE-S, which reveals that a strong interference between the work rate recovery potential by the ejector and the IHX exists. Furthermore, compared to that of a conventional transcritical $CO_2$ system, the compression ratio in the EJE-S is reduced 10.0%–12.1%, while that of the EJE-IHX-S is only reduced 5.6%–6.7%. Experimental results are used to indicate that the use of an IHX weakens the contribution of the ejector to the system performance.

## References

Aprea, C., Maiorino, A., 2008. An experimental evaluation of the transcritical $CO_2$ refrigerator performances using an internal heat exchanger. *International Journal of Refrigeration*, **31**(6):1006-1011. [doi:10.1016/j.ijrefrig.2007.12.016]

Boewe, D., Bullard, C., Yin, J., Hrnjak, P.S., 2001. Contribution of internal heat exchanger to transcritical R744 cycle performance. *International Journal of HVAC&R Research*, **7**(2):155-168.

Chen, Y., Gu, J.J., 2005. The optimum high pressure for $CO_2$ transcritical refrigeration systems with internal heat exchangers. *International Journal of Refrigeration*, **28**(8):1238-1249. [doi:10.1016/j.ijrefrig.2005.08.009]

Elbel, S.W., Hrnjak, P.S., 2004. Effect of Internal Heat Exchanger on Performance of Transcritical $CO_2$ Systems with Ejector. 10th International Refrigeration and Air Conditioning Conference at Purdue, West Lafayette, USA, Paper R166.

Elbel, S.W., Hrnjak, P.S., 2006. A Thermodynamic Property Chart as a Visual Aid to Illustrate the Interference between Expansion Work Recovery and Internal Heat Exchanger. 11th International Refrigeration and Air Conditioning Conference at Purdue, West Lafayette, USA, Paper R165.

Elbel, S.W., Hrnjak, P.S., 2008. Experimental validation of a prototype ejector designed to reduce throttling losses encountered in transcritical R744 system operation. *International Journal of Refrigeration*, **31**(3):411-422. [doi:10.1016/j.ijrefrig.2007.07.013]

Giuliani, G., Hewitt, N.J., Marchesi, D.F., Polonara, F., 1999. Composition shift in liquid-recirculation refrigeration systems: an experimental investigation for the pure fluid R134a and the mixture R32/134a. *International Journal of Refrigeration*, **22**(6):486-498. [doi:10.1016/S0140-7007(99)00009-2]

Hoegberg, M., Vamling, L., Bemtsson, T., 1993. Calculation methods for comparing the performance of pure and mixed working fluid in heat pump applications. *International Journal of Refrigeration*, **16**(6):403-413. [doi:10.1016/0140-7007(93)90057-F]

Kim, M.H., Pettersen, J., Bullard, C.W., 2004. Fundamental process and system design issues in $CO_2$ vapor compression systems. *Progress in Energy and Combustion Science*, **30**(2):119-174. [doi:10.1016/j.pecs.2003. 09.002]

Klein, S.A., Reindl, D.T., Brownell, K., 2000. Refrigeration system performance using liquid-suction heat exchangers. *International Journal of Refrigeration*, **23**(8): 588-596. [doi:10.1016/S0140-7007(00)00008-6]

Liu, S., 2008. Performance Study on an Ejector Used in $CO_2$-Heat Pump Water Heater. MS Thesis, Zhejiang University, Hangzhou, China, p.1-76.

Lorentzen, G., Pettersen, J., 1993. A new efficient and environmentally benign system for car air-conditioning. *International Journal of Refrigeration*, **16**(1):4-12. [doi:10.1016/0140-7007(93)90014-Y]

Mu, J.Y., Chen, J.P., Chen, Z.J., 2003. System design and analysis of the transcritical carbon dioxide automotive air-conditioning system. *Journal of Zhejiang University-SCIENCE A*, **4**(3):305-308. [doi:10.1631/jzus.2003.0305]

Robinson, D.M., Groll, E.A., 1998. Efficiencies of transcritical $CO_2$ cycles with and without an expansion turbine. *International Journal of Refrigeration*, **21**(7):577-589. [doi:10.1016/S0140-7007(98)00024-3]

Tao, Y.B., He, Y.L., Tao, W.Q., Wu, Z.G., 2010. Experimental study on the performance of $CO_2$ residential air-conditioning system with an internal heat exchanger. *Energy Conversion and Management*, **51**(1):64-70. [doi:10.1016/j.enconman.2009.08.024]